# Crack-free 30% Chromium-Nickel Alloy Welding Products for Nuclear Service

The final solution for crack-free welds in 30% Cr nickel welding alloy that meets significant acceptance criteria

Samuel D. Kiser[1,*],Brian A. Baker[2], Tao Dai[3], Yiyu Wang[3], Zhili Feng[3]

[1]*Special Metals Welding Products Co., Newton, NC 28658, USA*

[2]*Special Metals Corporation, Huntington, WV25705, USA*

[3]*Materials Science and Technology Division, Oak Ridge National Laboratory, Oak Ridge, TN 37831, USA*

## Abstract

Prior research work in the development of 30% Cr nickel alloy nuclear welding wires has resulted in the resolution of primary water stress corrosion cracking (PWSCC), ductility dip cracking (DDC), and improvement of solidification cracking (SC) resistance. The resolution to DDC exhibits some Laves phase, which has a negative effect on SC resistance. In this study, the use of an alternate carbide former, tantalum (Ta), in combination with niobium is researched. Three heats of recently designed Filler Metal 52MSS-Ta: HV1648, HV1673A, and VX131WXW were melted, fabricated, and systematically studied. DDC and SC were evaluated with thermodynamic modeling using the Scheil solidification simulation mode, two types of varestraint testing, and strain-to-fracture (STF) testing. The varestraint and STF testing results show an improved SC resistance with reduced Laves phase and concurrent excellent DDC resistance. Optimized compositions with low Laves phase also exhibit high Threshold Strain Values (TSV) in the STF test. VX131WXW which contains 2.81 wt.% Ta, 0.6 wt.% Nb and 6 wt.% Fe exhibits a TSV of 24%. Thermo-Calc computes the Laves phase to be 0.24% for VX131WXW compared to 0.06% Laves phase in HV1673A. This difference in Laves phase results in lower SC resistance of VX131WXW compared to HV1673A when measured with longitudinal varestraint testing (LVT). Maximum crack distance (MCD) for HV1673A is about 0.6 mm while that of Heat VX131WXW is about 1.0mm. The typical diluted weld deposit made with VX131WXW would also be resistant to PWSCC due to chromium content exceeding 24%. These simultaneous results mark progress toward crack-free welds and provide direction for further optimization of Ta-containing filler metals.

***Keywords***:30% Chromium-Nickel Alloy; Ductility Dip Cracking; Solidification Cracking; Strain-To-Fracture Testing; Thermodynamic Simulation; Characterization; Primary Water Stress Corrosion Cracking

## INTRODUCTION

Since the inception of nuclear power generation, nickel-chromium alloys and welding products have been employed for construction and repair of pressurized water reactor (PWR) internals wetted by primary water. After a brief trial with 304 stainless steel, base metal selection for nuclear construction was changed to Alloy 600 (UNSN06600). The welding products available for joining alloy 600 at that time were not capable of producing weldments with the desired integrity for nuclear service. Research into solidification cracking (SC), also known as “hot cracking”, in nickel-chromium-iron alloys started as early as 1946 (Ref. [1]). Early work conducted at the research laboratory of the International Nickel Company (INCO) in Bayonne, N.J. resulted in the development of welding products that became Welding Electrode 182 (AWS A5.11 ENiCrFe-3) and Filler Metal 82 (AWS ERNiCr-3) (Refs. [2], [3]). These were the first NiCrFe-type welding products capable of depositing crack-free and porosity-free weldments in Alloy 600. Further work at Huntington Alloys evaluated the cracking resistance of these products using varestraint testing methods (Ref. [4]). Much later, Alloy 600 was found to be subject to Primary Water Stress Corrosion Cracking (PWSCC) after long exposure to high purity reactor steam and primary water (Ref. [5]). As a result of PWSCC, Alloy 690 (UNS N06690) containing 30% chromium essentially replaced 600 for components of the PWR nuclear steam generator (Ref. [6]). To accomplish PWSCC-resistance in welds, the welding wire should contain about 29-30% chromium (Cr) and after moderate dilution, the weld deposit must have no less than 24% Cr to be acceptable as “corrosion resistant” against PWSCC in accordance with the American Society of Mechanical Engineers-Boiler and Pressure Vessel Code (Ref. [7]). Recently, Filler Metal

*Corresponding author, email: skiser@smwpc.com, phone: 828-461-5410

52MSS weld metal was tested by Pacific Northwest National Laboratory and found to have an acceptably low crack growth rate (CGR) of 1.0 x $10^{-9}$ mm/sec. (Refs. [8], [9])

The initial 30% Cr welding product designed for welding alloy 690 was Filler Metal 52 (AWS A5.14 ERNiCrFe-7). The Edison Welding Institute (EWI) claimed that Filler Metal 52 was more resistant to SC than Filler Metal 82 in their results of SC testing (Ref. [10]). Within the following decade, members of the U. S. Navy metallurgical and welding research team discovered what they called "cold cracking". Cold cracking was eventually associated with the "intermediate temperature ductility minimums" of Rhines and Wray (Ref. [11]). Following substantially more R&D efforts, cold cracking became known as ductility dip cracking (DDC). Since that time, a new generation of DDC-resistant 30%Cr welding products has been developed. The initial member of this family is Filler Metal 52M. Welds made with Filler Metal 52M have been shown to exhibit a PWSCC crack growth rate (CGR) better than Welding Electrode 182 (Ref. [12]). Filler Metal 52MSS was considerably superior to Filler Metal 52M in DDC resistance. When Filler Metal 52M was subjected to a European nuclear qualification testing program by AZZ, Filler Metal 52M was unable to meet the requirements. Filler Metal 52MSS was subjected to the same testing program and was successfully qualified. The detailed metallographic analyses of both sets of specimens disclosed remarkably clear results: Light Optical Microscopic examination (LOM) of multiple sections of identical welds deposited with each product revealed no DDC in Filler Metal 52MSS and no SC in Filler Metal 52M. In addition, the DDC cracks in Filler Metal 52M were approximately twice the length of the SC cracks found in Filler Metal 52MSS and there were fewer cracks in Filler Metal 52MSS [13]). Filler Metal 52M has no Laves and no SC with a narrow delta-T solidification cracking range (SCR, 123 °C), while Filler Metal 52MSS has SC compromised by Laves (0.67%) and a considerably wider delta T of 224 °C. Prior metallurgical observation showed Filler Metal 52M to have straight grain boundaries and DDC and Filler Metal 52MSS had tortuous grain boundaries (Ref. [14]) and no DDC. These observations confirm that the next objective was to resolve SC in Filler Metal 52MSS. While the performance of Filler Metal 52MSS (NX79W1UK) was better than that of Filler Metal 52M, it contained some Laves phase shown in a previous work performed by Lehigh University (Ref. [15]). Lehigh's SEM investigation of the crack tip area of a longitudinal varestraint testing (LVT) test sample directly implicated Laves phase in initiating the LVT cracking (Ref. [15]). Note the areas of increased niobium (Nb) and (Mo) in the Laves Phase. The European nuclear qualification test above used the parameter optimization results of the STF test by Kreuter (Ref. [16]) to select the most DDC-resistant heat of Filler Metal 52M for the qualification test.

Filler Metal 52 has been found to be susceptible to SC, DDC and other welding related issues, such as oxide formation and oxide inclusions (Ref. [17]). When Cr was raised to 30% to mitigate PWSCC, it decreased solubility for other elements and drove the filler metals closer to the long-range-order (LRO)-inducing ratio of $Ni_2Cr$, an unwanted ordered phase (Ref. [18]). This also made the filler metal more likely to form long straight grain boundaries which are susceptible to DDC. To counter straight grain boundaries, Nb and Mo additions were discovered to precipitate and deploy a wide dispersion of pre-solidification niobium carbides (NbC) that pinned migrating grain boundaries after solidification and created tortuous grain boundaries (Refs. [14], [19]). The key to providing the effective level of serpentine grain boundaries was found to be governed by an appropriate addition of Mo to the 30% Cr nickel alloy weld wire that contained about 0.03% carbon (C) and 2.1 to 3.0% Nb. The addition of about 3-4% Mo to niobium-containing ERNiCrFe-13 filler metals regulates the morphology and deployment of the MC carbides (NbC) that precipitate first from the molten weld pool. These carbides are formed early in the solidification process and are relegated to the interdendritic areas where they provide precipitates that pin later migrating grain boundaries and induce grain boundary tortuosity (Refs. [14], [19]). However, the 9% iron (Fe) that was necessary to forestall LRO in alloy 690 base metal creates conditions in weld metal that contains Nb which result in a terminal eutectic Laves phase which compromises SC resistance. One of the novel findings of this current research is that the tendency for Laves phase to compromise SC resistance was reduced by replacing Nb with tantalum (Ta) while maintaining Mo to influence carbide behavior. The beneficial effect of Ta on SC resistance will require additional research, but it is most likely related to the narrower solidification temperature range (STR) provided by Ta pointed out by Hope and Baeslack et.al. (Refs. [20], [21]). Also, with the additional elements of Nb, Ta, and Mo, the 2:1 ratio of Ni-to-Cr is disrupted so that LRO is discouraged (Ref. [16]).

Multiple efforts have been made to study SC and DDC over the past two decades. There have been many SC resistance tests, including transverse varestraint testing (TVT) and longitudinal varestraint testing (LVT). Several important discoveries have been made while pursuing better cracking resistance. The Strain-to-Fracture (STF) test may be the most significant new welding research tool to have been developed during the last several decades. Before the STF test, invented by Nissley and Lippold (Ref. [22]), nearly all cracking in the austenitic nickel alloys was referred to as "microfissuring" (Ref. [11]). Now it is possible to study and measure SC associated with liquid phase separately from DDC that occurs in the solid state. For the 30% Cr nickel alloy welding products, the best SC resistance is obtained with tight control of low-melting-temperature tramp elements such as sulfur (S), phosphorus (P) and lead (Pb) and the minimization of Laves phase, a terminal eutectic phase that contains enriched areas of Nb, Mo and others (Ref. [15]). Experimental work involving Ta began in 2012 with the melting of a Ta-containing heat of Filler Metal 52MSS-Ta (HV1648) and continued as various ratios of Ta and Nb were explored (Refs. [23], [24], [25]). More recently, Fusner et al. (Ref. [26]) explored filler metals involving Nb and Hf using computational and experimental techniques. Among other significant findings, Nb was found to increase the

solidification temperature range and contribute to SC tendency. STR, PWSCC, DDC and varestraint testing were reported on Filler Metal 52MSS and experimental filler metals by Kiser et al. (Ref. [25]). Outstanding TSV for NX79W1UK was found to be 19% in this research. Hope and Lippold continued their study of alternative carbide formers by testing Hf and Ta-containing filler metals. It was concluded that the Hf-containing filler metals suffered from the SC, but the Ta-containing filler metals showed more promise, but still only 10% TSV in the STF test (Ref. [20]).

From this point, a simultaneous solution to SC and DDC was needed that would provide TSV of 15% (Ref. [27]) in the STF test and an MCD of between 0.6mm and 1.0mm in varestraint testing. A solution was expected using a combination of Nb and Ta. Modeling was used to guide the filler metals to be tested in minimizing Laves phase and optimizing SC resistance by varestraint testing and minimizing DDC by STF testing. In this work, DDC and SC resistance of a recently designed Filler Metal 52MSS-Ta were evaluated with LVT, TVT, and STF tests. Solidified phases and typical microstructure of three heats were predicted and observed with thermodynamic simulation and metallurgical characterization. A comparison of historically developed alloys with the current Filler Metal 52MSS-Ta were conducted to analyze the DDC and SC resistance mechanism.

## EXPERIMENTAL PROCEDURES

### Thermodynamic Modeling

In this work, thermodynamic modeling with the Thermo-Calc (TCNI8 database) was conducted to predict the critical solidification and phase transformation temperatures, the phase percentages of gamma, eutectic, Laves, and other phases across multiple analyses. The compositions used for the Scheil solidification modeling are shown in Table 1. The Scheil solidification simulation predicts key temperature parameters, MC carbides, and Laves phase percentages at the formation of 99% solid.

### Varestraint Testing

Both transverse varestraint testing (TVT) and longitudinal varestraint testing (LVT) were conducted. TVT parameters were: 180 amps DCEN at 10 volts, 0.08” arc length and 5 in/min. travel speed. For the LVT, essentially undiluted specimens were produced, and composition was verified by spectrographic technique. Table 2 presents the chemical composition verification of 8 specimens for heat number VX131WXW. The specimen dimensions were ¼” x 1” x 6”. The testing parameters were 125 amps DCEN at 10 volts at travel speed 6 inch/min and arc length of 0.07”- 0.10”. The quantity “maximum crack distance” (MCD) is the defining parameter for a test or sequence of tests. It is defined as the maximum crack length after strain saturation has been reached, which is usually between 3% and 5% strain. Strain saturation is reached when further strain fails to produce larger cracks. The MCD after strain saturation was measured after TVT and LVT (Ref. [18]).

### Strain-to-Fracture Testing

To perform STF tests, an electromagnetic stirring coil was fabricated to produce flat, stirred spot welds following the prior work of Nissley (Ref. [27]). These spot welds create 360 degrees of radial dendrites and were made on both sides of each sample to create maximum data per test. Table 3 lists the chemical compositions of the filler metals STF tested. Table 4 provides the GTAW spot welding parameters used for fabricating the STF specimens. The 0.25” thick specimen geometry and dimensions are shown in Figure 1. The STF test was conducted using a Gleeble® 3500 testing machine capable of heating metallic samples that contain spot welds to a specified temperature and then imposing a predetermined strain on the gauge length of the sample. Figure 2 illustrates a typical thermal-mechanical history of a STF test. By correlating strain versus the amount and size of cracking it is possible to determine the hot ductility capacity of weld metal and from that then to determine the threshold strain value (TSV). The TSV is the maximum strain at which no cracking occurs. After spot welding, the spots were surface ground smooth and flat and were loaded into the Gleeble® machine and tested according to the parameters given in Table 5, based on previous work by Kreuter (Ref. [16]). Figures 1c and 1d show the samples after the STF testing; it is noted that the samples have undergone tremendous strain at 950 °C. Next, the tested samples are observed at 30X magnification on a LOM where cracks are measured, counted, and recorded. These threshold strain values (TSV) are used to characterize the DDC cracking resistance of deposited weld metals being tested.

### Microstructure Characterization

Scanning electron microscope (SEM) and energy dispersive X-ray spectroscopy (EDS) were used to analyze carbides and their compositions of the spot weld specimens after a mechanical polishing. Optical microscope and electron backscatter diffraction (EBSD) mapping were used to show the grain boundaries in the spot weld of a typical specimen. Spot welds right after the STF were observed under optical microscope for crack measurements.

## RESULTS

### Thermodynamic Modeling

Figure 3 presents the Scheil simulation results by Thermo-Calc. The predicted critical solidification temperatures and secondary phase fractions are tabulated in Table 6. Filler Metal 52M, NX77W3UK, and NX79W1UK are all existing filler metals that have been used in nuclear welding while Filler Metal 52MSS-Ta experimental heats HV1648, HV1673A and VX131WXW were investigated for studying effects of Ta additions. The solidification temperatures and fraction of MC phase are similar, but the fraction of Laves phase is quite different among the six compositions. It is known that the Laves percentages are the major factors that control SC in these "ultra-clean" (very low impurity) filler metals. It is noted that the very low percentages of Laves phase in HV1673A and Filler Metal 52M result in very good TVT performance (Ref. [18]), as shown in Figure 4. This indicates there is a very low likelihood of SC in Filler Metal 52M and Filler Metal 52MSS-Ta when no Laves phase is present in the microstructure. Therefore, the best solidification sequence is Gamma phase → MC → solid. Overall, in these very "clean" nuclear grade filler metals, SC is expected to be mainly influenced by the amount of Laves phase present after solidification. Comparing Filler Metal 52M with HV1673A, it appears that the source of low Laves in Filler Metal 52M is mainly very low Mo and controlled Nb in the presence of Fe contents while in HV1673A it is the presence of very low Fe co-present with <1.0 wt.% Nb. Because 3-5 wt.% Mo is required for tortuous grain boundaries that prevent DDC, and that PWR nuclear applications that require welding often include iron-based alloys, iron dilution cannot be avoided. Therefore, because low iron in weldments cannot be assured and Mo is necessary, minimization of Nb seems to be called for with a substitute carbide former such as Ta.

### Varestraint Testing.

Based on modeling results, three melts (heat numbers: HV1648, HV1673A, VX131WXW,) were fabricated with varying amounts of Fe, Nb, and Ta as shown in Table 1. LVT and TVT showing the SC resistance of the three melts are compared in Figure 4 and Figure 5. Previous results of Filler Metals 52MSS, 52i, and 82 (Refs. [18], [28]) are also shown in the Figures for comparison. Figure 4 shows the TVT results that compare Filler Metal 52M (0.0% Laves) with Filler Metal 52MSS-Ta (HV1673A) (0.06% Laves). It is not unusual to have a good SC resistance with low Laves for both filler metals, but the absence of sufficient Nb and no appreciable Mo in Filler Metal 52M minimizes the formation of NbC and allows the formation of long straight grain boundaries which are subject to DDC. Filler Metal 52MSS-Ta (HV1673A) exhibits a very low MCD value of 0.6 mm in the TVT tests and is corroborated in the LVT tests. Figure 5 compares the LVT results of several heats of Filler Metal 52MSS-Ta and Filler Metal 52MSS with Alloy 625 (Refs. [18], [29], [30]). It is obvious that the Alloy 625 shows the largest MCD (1.6 mm), HV1648 has a lower MCD (1.1 mm), while VX131WXW has a MCD of .9-1.0 mm and (HV1673A) exhibits the lowest MCD of (0.6 mm). These comparisons indicate that HV1673A (Filler Metal 52MSS-Ta) has the highest resistance to SC. The best performances observed are about 0.6mm MCD measured in Filler Metal 52M (0% Laves) and experimental HV1673A Filler Metal 52MSSTa (0.08% Laves) with very low impurities. LVT results that compare HV1673A with NX79W1UK (0.57% Laves), VX131WXW (0.24% Laves), and alloy 625 are shown in Figure 5, (the two bottom curves are Filler Metal 52MSS-Ta). LVT data usually compare favorably with TVT data except when occasional scatter occurs. All these products deposit high-quality welds and the positions of the cracking performance curves correlate well with their percentages of Laves phase of each.

### Strain-to-Fracture Testing

The STF testing results for VX131WXW at 950 °C are summarized in Table 7. The threshold strain value (TSV) is the highest strain sustained without cracks or major cracking. "Without cracks or major cracking" is the terminology used by the designers of the STF test (Refs. [22], [23]). The chosen samples in this study strained below the TSV are crack-free to minimize debate. 24.19% TSV recorded for sample 29-39 is quite good and even surpasses the TSV of that of heat NX79W1UK, which was the previous best STF performance of any of the 30% Cr wires (Refs. [23],[31]). From Table 7, it is noted that samples 23-33, 25-35, and 29-39 are all crack-free, and were tested at 19.18%, 22.66% and 24.19% strain. These results indicate the TSV for VX131WXW is greater than 24%, and that three values for this weld metal averaged over 20% indicating repeatability of the noteworthy performance. Figure 6 shows a typical example of the crack-free STF specimen (spot weld #39) after testing. For comparison, the TSV for Filler Metal 52 is only 3% and the TSV for Filler Metal 52M is 9%. Range of values for Filler Metal 52M from 5% to 9% are reported by Kreuter (Ref. [16]) and vary because three different specimen preparation methods were used with three different heats of wire. Chemical compositions of wire and specimen preparation methods are disclosed in Reference [16].

The MC fractions shown in Table 6 suggest that the MC phase precipitates may counteract DDC. If the MC carbides precipitate while the pool is molten, and if they are of appropriate size and are widely distributed, they contribute to tortuous grain boundaries which resist DDC (Ref. [32]). Figures 7a and 7b show the tortuous grain boundaries of spot weld 40 of the heat VX131WXW. EBSD analyses in Figures 7c and 7d show more details of similar tortuous boundaries from NX79W1UK. This resistance occurs because the solidification grain boundaries tend to move or migrate as solidification stresses begin to develop. The pre-placed high melting temperature MC precipitates can pin these moving grain boundaries and force them to become circuitous rather than long and straight as are often seen in welds made with Filler Metal 52 and Filler Metal 52M. The SEM and EDS analyses

in Figure 8 show an example of the Ta/Nb carbides distributed along the tortuous grain boundaries. These tortuous grain boundaries shown in Figure 8b tend to reduce the tendency for grain boundary sliding and thus reduce the tendency for DDC to occur (Ref. [33]). Figure 9 compares the current STF data with the early 52 filler metals and Filler Metal 52M data from Kreuter's work (Ref. [16]). Also shown are the seminal data of 3W1, 3W2, 3W3 and 3W4 (Ref. [23]) that illustrate the progressive effectiveness of %Mo as it approaches and exceeds 3% in conjunction with Nb to form tortuous grain boundaries and provide increasing DDC resistance. From the data presented for 3W1 through 3W4 there appears to be a trend that 3-4%Mo in Filler Metal 52MSS and Filler Metal 52MSS-Ta is needed to form effective carbide networks that result in tortuous grain boundaries. This trend seems to be supported by Hope's finding of only 10%TSV in the Mo-free "Ni-30Cr-8Fe-4Ta-0.04C" (Ref. [20]) These levels of Mo do not appear to participate in MC nor $M_{23}C_6$ (Ref. [34]), but increasing Mo seems to discourage the formation of $M_{23}C_6$ ((Ref. [14], [19]). Finally, the most recent entrant to the family of nickel-chromium welding alloys, Filler Metal 52MSS-Ta, VX131WXW is represented by its TSV value of 24% at the top right of the chart.

## DISCUSSION

To optimize DDC cracking resistance of ERNiCrFe-13, tortuous migrated grain boundaries are required. These are generated by additions of 0.03%C, 3% to 4%Mo and 3% to 4% combined Nb + Ta (Ref. [14]). NX79W1UK exhibited excellent DDC resistance (Table 1) except it contained Laves phase which compromised SC resistance (Table 6). Figure 9 depicts a plot of 19 TSVs from STF test data points. It is noted that the abscissa has numerical values that represent the totals of weight percent of Mo + Nb + Ta for each filler metal. The data with 10% or less TSV were made with filler metals that contained less than 2% Mo. When ERNiCrFe-13 compositions contain 3% to 4% Mo, and about 0.03% C, MC (Nb and\or Nb+Ta) carbides are formed and are distributed sufficiently to produce tortuous grain boundaries as described in Results section and shown in Figure 7. It is proposed that appropriate tortuosity allows spot welds in these filler metal specimens to sustain considerably higher TSVs than those with less Mo without cracking when tested at 950 °C. From the early work by Lippold and Ramirez (Ref. [34]), it appears that Mo does not participate in the carbide formations and appears to influence only the size and distribution of the carbides that cause tortuosity of the grain boundaries. It is further proposed that insufficient Mo fails to initiate effective carbide networks to create tortuous grain boundaries. Comparing NX77W3UK with NX79W1UK in Table 3, the two are almost identical. It may be concluded that the former (NX77W3UK) has sufficient Mo but insufficient carbon (0.023%) to form an appropriate carbide network and only exhibits TSV of 16% but still meets criteria of 15% by Nissley (Ref. [27]). The latter (NX79W1UK) contains sufficient carbon and Mo to form a more efficient carbide network and exhibits a higher TSV of 19% to 21% (Refs. [23], [28]). Note that both filler metals contain very low levels of S and P while sustaining high TSV values. A prior work by Fusner et al. (Ref. [26]) states "Recent testing at The Ohio State University (OSU) has shown that extremely low S and P caused an increase in DDC." Current testing of Filler Metal 52MSS and Filler Metal 52MSS-Ta, both NX79W1UK and VX131WXW, exhibit TSV in STF testing of over 20% and both have extremely low S and P (See Table 1 and Figure 9). Both have <0.00016 wt.% S and <0.006 wt.% P. These low levels of S and P are important to SC resistance and the test results seem to be inconsistent with DDC claims of Fusner, et al (Ref. [26]).

Finally, VX131WXW has 2.81 wt.% Ta and 0.61 wt.% Nb (to control Laves effects for SC resistance), when STF tested at Oak Ridge National Laboratory, it exhibited a TSV of 24%. All three compositions, NX77W3UK, NX79W1UK, and VX131WXW contain between 3 and 4 wt.% Mo which is responsible for the efficient carbide networks that sustain high TSV values. These compositions exhibit 1.5X to 2.5X higher TSV than the result of Mo-free 10% TSV for Ni-30Cr-8Fe -4Ta-0.04C described by Hope and Lippold (Ref. [20]). VX131WXW also has very low S and P to help deliver good SC results and do not seem to compromise STF TSV values. Comparing predicted modeling results (Table 6) for VX131WXW with those for NX79W1UK it shows 0.24% Laves for the former and 0.67% for the latter. This difference in predicted Laves results in MCD values of 1.2 millimeters for both TVT and LVT of NX79W1UK in Figures 4 and 5 vs MCD of 1.0 mm for VX131WXW in Figure 5 for LVT. Magnitude of difference is not pronounced, but direction agrees with the proposed theory. Much lower predicted values for Laves phase for Filler Metal 52M and HV1673A align themselves with even lower MCD for both Filler Metal 52M and HV1673A in Figures 4 and 5. TVT values for both filler metals are shown in Figure 4 as MCD 0.6 mm and for HV1673A in Figure 5 MCD and LVT is corroborated at 0.6 mm. Continued optimization work on VX131WXW is predicted to minimize Laves phase and to improve SC results to approximately 0.6 mm to 0.8 mm MCD without compromising measured 24% TSV in STF testing. Acceptable values for crack growth rate in PWSCC testing is expected due to 30 wt.% Chromium in each of the filler metals, but actual testing can be used to confirm.

## Conclusions

In this work, ductility dip cracking and solidification cracking resistance of three heats of Filler Metal 52MSS-Ta (AWS A5.14, ERNiCrFe-13) were systematically studied via thermodynamic modeling, varestraint testing and strain-to-fracture testing. The main findings can be summarized as follows:

1. With the addition of Ta and optimized Mo content, Filler Metal 52MSS-Ta exhibits improved DDC and SC resistance simultaneously.
2. Strain-to-fracture testing results show very low levels of S and P have no negative effect on DDC resistance in the filler metals tested.
3. The highest STF Threshold Strain Value for Filler Metal 52M of 9% is consistent with the TSV of 10% for Ni-30Cr-8Fe-4Ta-0.04C as neither have significant Mo additions. Clearly 3- 4 wt.% Mo is necessary to achieve very high TSV's (18%-24%) in Filler Metal 52MSS-Ta and Filler Metal 52MSS. However, excess Mo and Nb/Ta can contribute to formation of Laves phase. Levels of both Mo and carbide formers depend on wt.% C content. Modeling and testing of compositions with lower levels of both Mo and carbide formers (and combinations) is needed for further optimization
4. TVT and LVT testing of HV1673A and TVT testing of Filler Metal 52M show MCD values of 0.6mm for these two filler metals which have no Laves phase predicted by ThermoCalc. VX131WXW produced a TSV in STF testing of 24% at 950 °C. and an MCD of 1.0mm in LVT testing with a predicted Laves phase of 0.24% mole fraction. It is expected that this SC MCD result can be improved with further optimization/minimization of Laves phase.
5. Because Fe dilution cannot be avoided in many pressurized water reactor welding applications, a major addition of Ta is needed to be added to ERNiCrFe-13 to achieve crack resistance goals desired.
6. Exceptional TSV's are achieved in STF testing of Filler Metal 52MSS-Ta and Filler Metal 52MSS at 950 °C with an addition of 3-4 wt.% Mo. STF results show 6 data points with 13% through 24% TSV for welds that contain more than 3 wt.% Mo while those with lower Mo levels have less than 10% TSV.

## Acknowledgments

We are grateful to the Oak Ridge National Laboratory (ORNL), our co-authors, and Doug Kyle also of ORNL who provided welding technology and support for our program. We are thankful for extensive technical support in STF testing protocols and techniques provided by Dr. Nathan Nissley of EXXON-Mobil and we appreciate Jeff Enneking of Framatome, Lynchburg, Va. who fabricated the 20 mm alloy 690 plate from which we took STF specimens. Also, we are grateful to the DOE office of Nuclear Energy, Advanced Reactor Technologies Program for their very helpful support. We also recognize Special Metals Welding Products Company for supplying the alloy 690 plate and Filler Metal 52MSS-Ta that were used to fabricate the STF specimens.

## References

[1] T.E. Kihlgren, C.E. Lacy. The Control of Weld Hot Cracking in Nickel-Chromium-Iron Alloys. Welding Journal Research Supplement, December,1947.
[2] W.A. Fragetta, G.R. Pease. The Welding of INCONEL for Nuclear Power Application. Welding Journal Research Supplement, April 1959.
[3] C.E. Witherall. Welding of Nickel-Chromium-Iron Alloy for Nuclear-Power Stations. Welding Journal Research Supplement, November 1960.
[4] A.C. Lingenfelter. A Study of Segregation in INCONEL-Type Alloy Weld Metal Structures. Master Thesis, University of Cincinnati, 1974.
[5] U.S. Nuclear Regulatory Commission, Office of Nuclear Reactor Regulation, "Primary Water Stress Corrosion Cracking (PWSCC) of INCONEL 600," 1990. Information Notice No. 90-10.
[6] S.D. Strauss. INCONEL 690 is alloy of Choice for Steam Generator Tubing, Power, February 1996.
[7] ASME Boiler and Pressure Vessel Code, Section XI, Code Case N740, Winter Edition, 2013.
[8] M. Toloczko. Update on PNNL Crack Growth Research on alloy 152, Filler Metal 52M and UNS N06055 alloy- Part I. EPRI-NRC Meeting November 2011, Tampa, FL.
[9] M. B. Toloczko, M. J. Olszta, S. M. Bruemmer, Stress Corrosion Crack Growth of Alloy Filler Metal 52M in Simulated PWR Primary Water. Proceeding of 15th International Conference on Environmental Degradation in Nuclear Power Systems-Water reactors. Editor: J. T. Busby, G. Illevbare and P. L. Andresen, The Minerals, Metals and Materials Society, 2011, p.225.
[10] B.B. Hood, W. Lin. Weldability of INCONEL Filler Materials. 7th International Symposium on Environmental Degradation of materials in Nuclear Power Systems, August 6-10, 1995, Breckenridge, CO.
[11] F.N. Rhines, P.J. Wray, Investigation of the Intermediate Temperature Ductility Minimum in Metals. Transactions, ASM, Vol.54, 1961, page 117-128.
[12] R.J. Jacko, R.E. Gold. Comparative PWSCC Crack Growth Rate Studies of Alloy Filler Metal 52M and Alloy 182 Weld Metals. EPRI Conference on PWSCC of Alloy 600, March 7-10, 2005, Albuquerque, NM.

[13] P. Lester, M. Keller, D. Barborak, S. Vancluysen. The Testing of ERNiCrFe-13 for Use in Structural Weld Overlays. The 11th International EPRI Conference for Welding and Repair Technology for Power Plants, June 26, 2014, Naples, FL.
[14] S.D. Kiser, B.A. Baker, D.E. Waskey. Welding Alloy and Articles for use in Welding, Weldments and Method for Producing Weldments. U.S. Patent No. 8,187,725, Publication No. 20100136368 A1 2010-06003, June 3, 2010.
[15] J.N. Dupont, Lehigh University, privately funded research into Laves phase effects on LVT performance, 2016
[16] V.C. Kreuter. Optimization and Application of the Strain-To-Fracture Test for studying Ductility-Dip-Cracking Nickel-base alloys for Filler Metals. Master Thesis. Ohio State University, 2015
[17] B. Newton, S. Kiser. Alloy 52 vs Filler Metal 52M Which is Better for Structural Weld Overlays?. EPRI Conference: Nuclear Welding and Repairs Workshop, 2006.
[18] S. McCracken. Welds and Mockups. EPRI Collaborative Meeting on Alloy 690/52/152 PWSCC Research, December 4, 2019, Tampa, Florida
[19] J.C. Lippold, N.E. Nissley. Ductility Dip Cracking in High Chromium, Ni-Base Weld Metals. Second International Workshop of Hot Cracking Phenomena in Welds, Berlin, Germany, March 5-6, 2007.
[20] A. Hope, J. Lippold. Development and testing of a high-chromium, Ni-based filler metal resistant to ductility dip cracking and solidification cracking. Welding in the World, 2017, 61:325-332
[21] W.A. Baeslack III, S.L. West, T.J. Kelly. Weld cracking in Ta-modified cast Inconel 718. Scripta Metallurgica, 1988, 22(5):729-734.
[22] N.E. Nissley, J.C. Lippold. Development of the strain-to-fracture test for evaluating ductility-dip cracking in austenitic alloys. Welding Journal, 2003, 82(12):355s-364s.
[23] R. Zhang, M. Caruso, S. Kiser, J. Crum, J. Forrester. New 30%Cr-Containing Ni-Cr-Fe Welding Product Provides Outstanding Resistance to PWSCC, Ductility Dip Cracking (DDC), and Meets All Other Nuclear Welding Requirements. CORROSION 2012; Paper No. C2012-0001743, March 11–15, 2012, Houston, Texas.
[24] S. Kiser, M. Caruso, B. Baker. Further Characterization of UNS N06055 Nuclear Welding Product, CORROSION 2016, Paper No. 7296, March 2016, San Diego, CA USA
[25] S. Kiser, M. Caruso, R. Zhang, B. Baker. Development and Characterization of UNS N06055 Nickel Alloy Welding Product, CORROSION 2014 Paper No. 4223, March 9-13, 2014, San Antonio, TX, USA
[26] E. Fusner, A. Hope, J. Lippold. Development of High-Cr, Ni-bsed Filler Metals using combined computational and experimental techniques. Welding Journal, 2014, 93 (5): 1715-182s
[27] N.E. Nissley. Development of the Strain-to-Fracture test to study Ductility-Dip Cracking in austenitic alloys. Master Thesis, Ohio State University, Columbus, 2002.
[28] B. Alexandrov, A. Hope, B. Sutton, J. Lippold, S. McCracken. Weldability of High Chromium Nickel-Base Filler Metals for Nuclear Power Applications. Second International EPRI Conference, Orlando, FL. June 21-24, 2011
[29] B. Alexandrov, J. Lippold, J. Sowards, A. Hope, S. McCracken. Weldability of Nickel-based Alloys for Nuclear Power Applications. AWS Professional Program, November 18, 2009, Chicago, IL.
[30] S. McCracken, Welding Mockups, presentation at EPRI-NRC Collaborative Meeting on Alloy 690/52/152 PWSCC Research November 28-Dec2, 2011, Tampa, FL.
[31] N.E. Nissley, J.C. Lippold. Further investigations of ductility-dip cracking in high chromium, Ni-base filler metals. Welding in the World, 2007, 51(9): 24-30.
[32] J.N Dupont, J. C Lippold, S.D. Kiser. Welding Metallurgy and Weldability of Nickel-Base Alloys. John Wiley and Sons, Inc., Hoboken, NJ, 2009.
[33] F. Noecker, J. Dupont. Metallurgical Investigation into Ductility Dip Cracking in Ni-based Alloys: Part II. Welding Journal, 2009, 88(3): 62s- 77s.
[34] J. Lippold, N. Nissley, A. Ramirez, C.R.M. Afonso. Evaluation of DDC in High-Chromium, Ni-base Filler Metals using the Strain to Fracture Test. Fifth International EPRI Conference for Welding and Repair Technology for Power Plants, June 2008.

**Figures:**

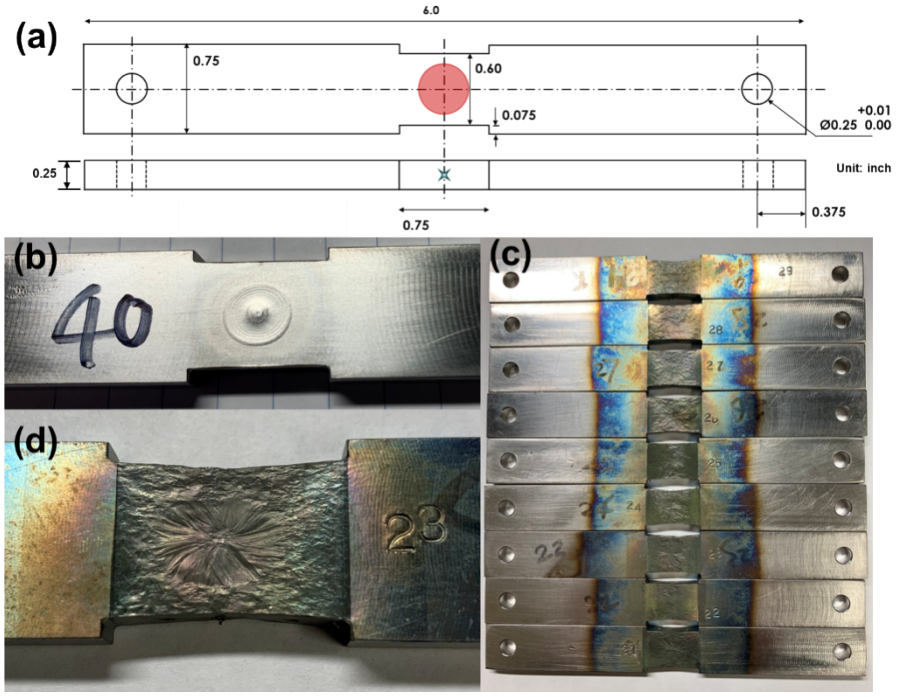


*Figure 1: (a) STF specimen geometry and dimension; (b) An example of the STF specimen before testing; (c) The STF specimens after testing; (d) magnified image of the STF specimen after testing.*

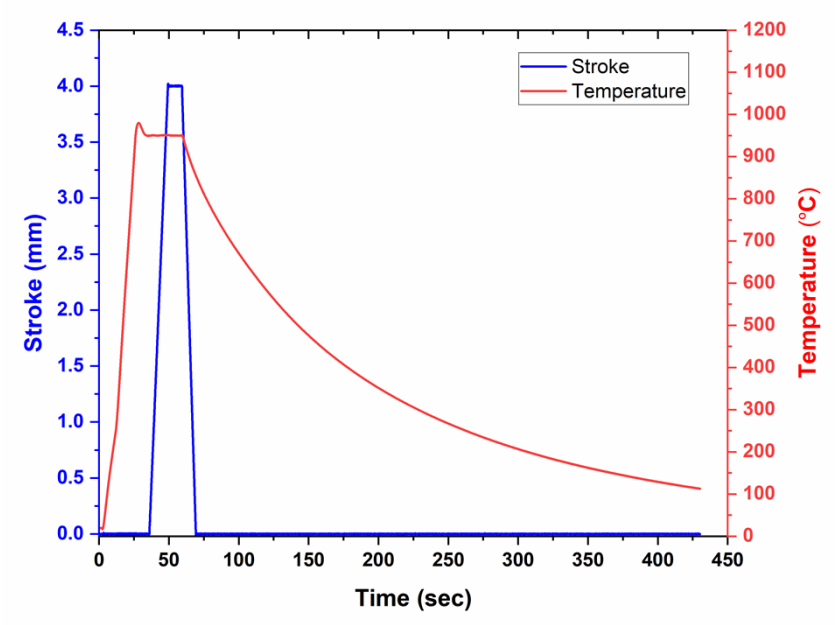


*Figure 2: A typical Gleeble thermal-mechanical history of the STF testing.*

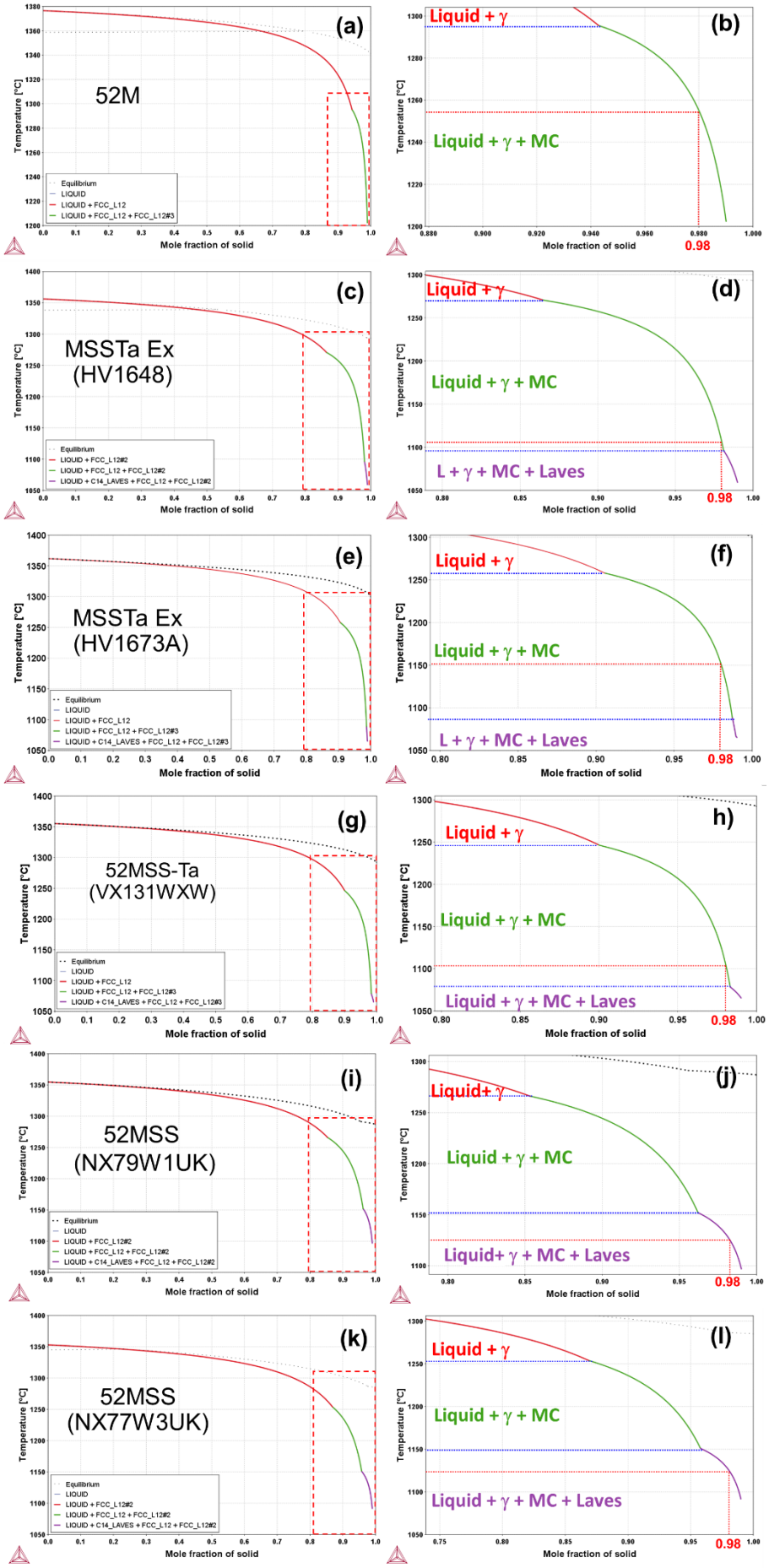


*Figure 3: Scheil solidification paths simulated by Thermo-Calc for alloys Filler Metal 52M, Filler Metal 52MSS, Filler Metal 52MSS-Ta and MSSTa Ex*

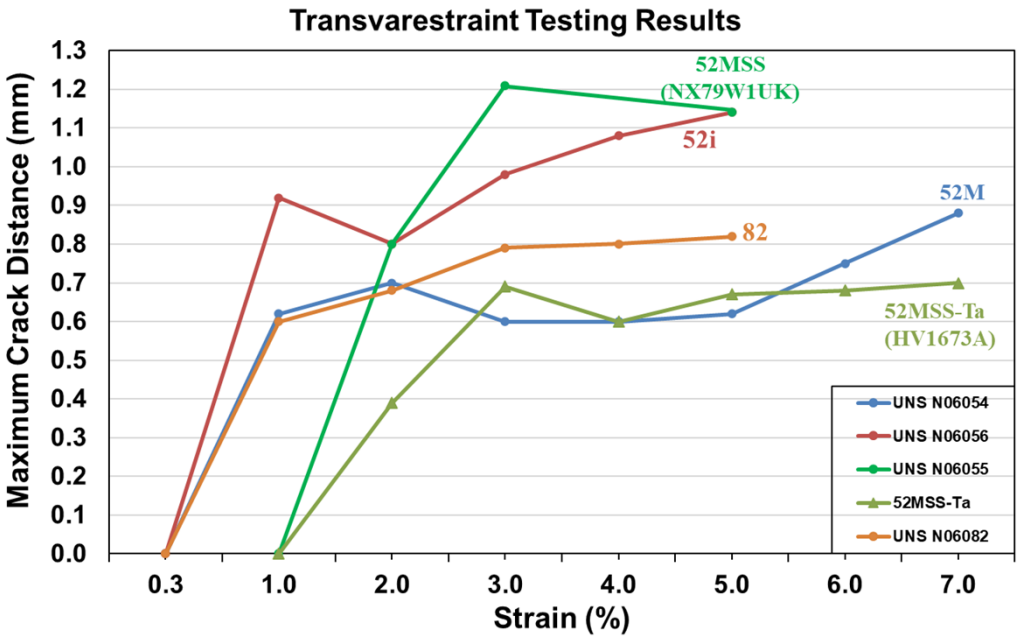


*Figure 4: Comparison of transvarestraint testing results among Filler Metal 52M, Filler Metals 52MSS,52i, 82 (Ref. 30) and Filler Metal 52MSS-Ta*

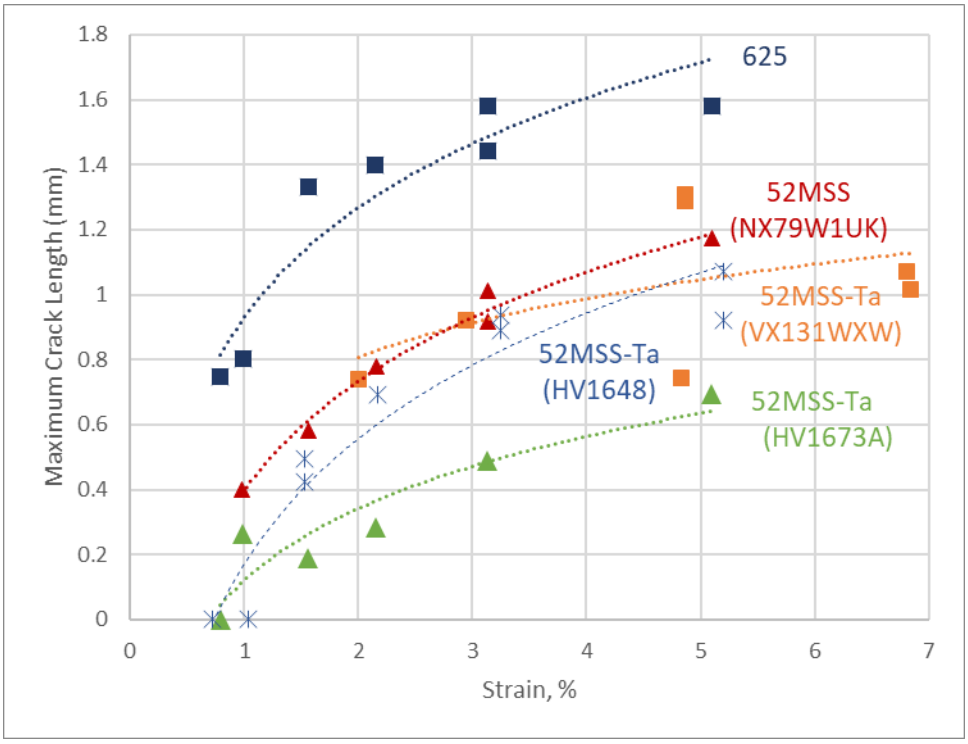


*Figure 5: Comparison of longitudinal varestraint testing among the Alloys 625 (Ref. 29), Filler Metal 52MSS (Ref. 30) and various Filler Metal 52MSS-Ta*

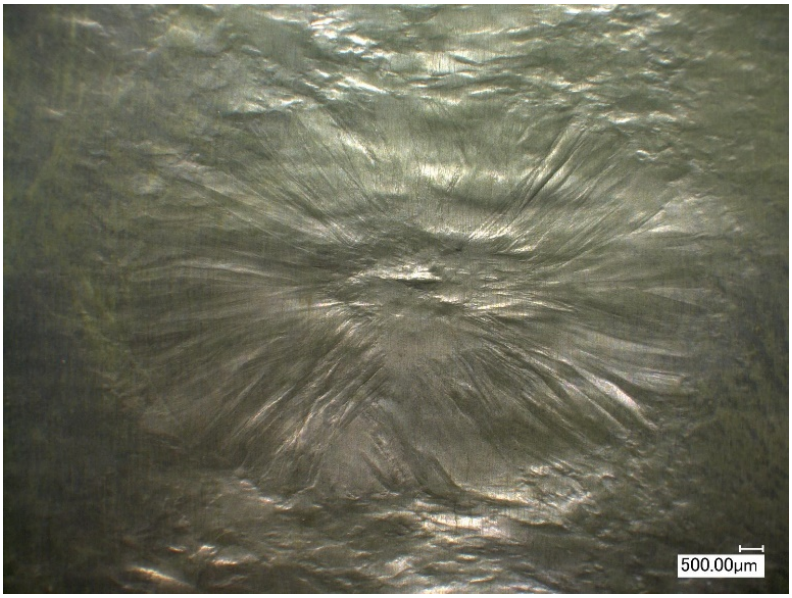


*Figure 6: Optical image (X30) showing the crack-free STF specimen (#39) after testing*

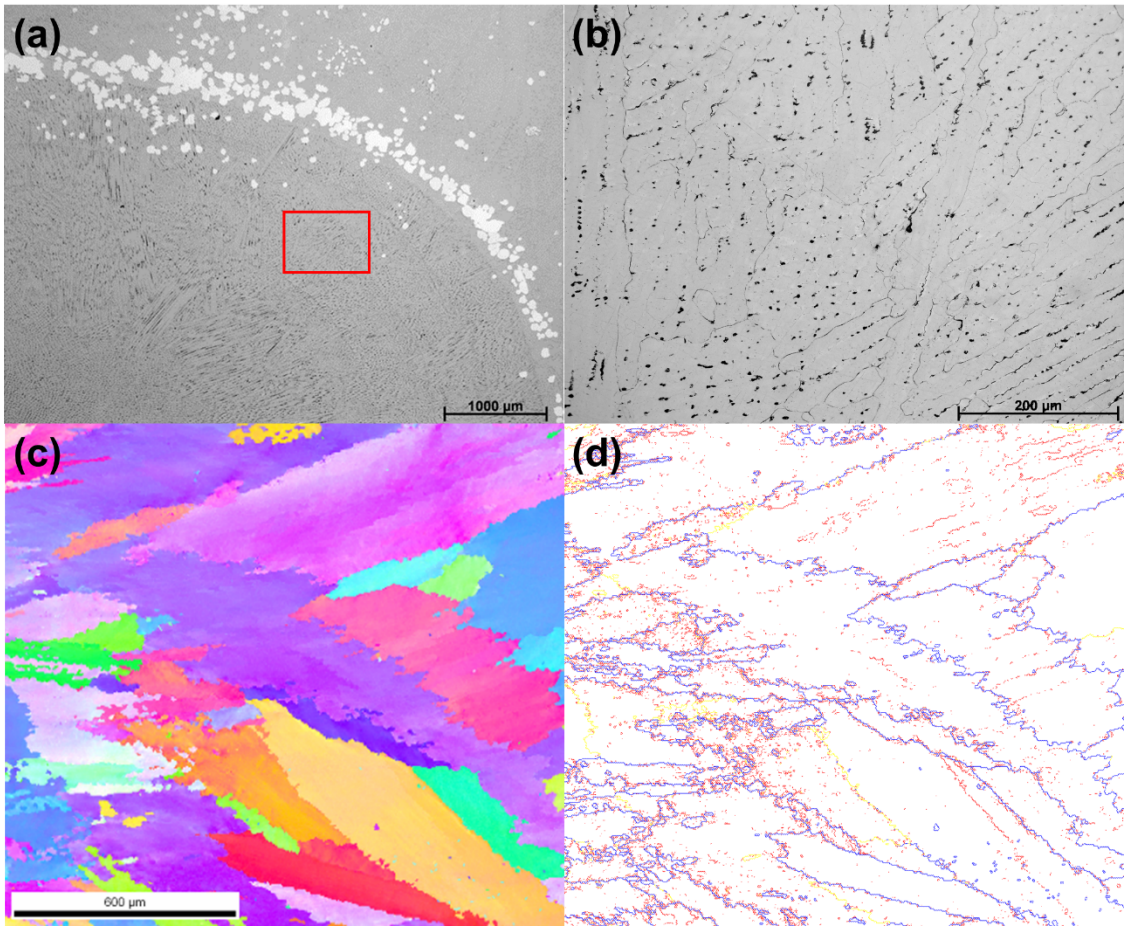


*Figure 7: Optical images and EBSD maps show tortuous grain boundaries in specimens after STF testing. Filler Metal 52MSS-Ta spot weld #40: (a) optical image, (b) optical image of the region highlighted by the red box in (a). Filler Metal 52MSS specimen: (c) inverse pole figure (Ref. 14), (d) grain boundary map (Ref. 14).*

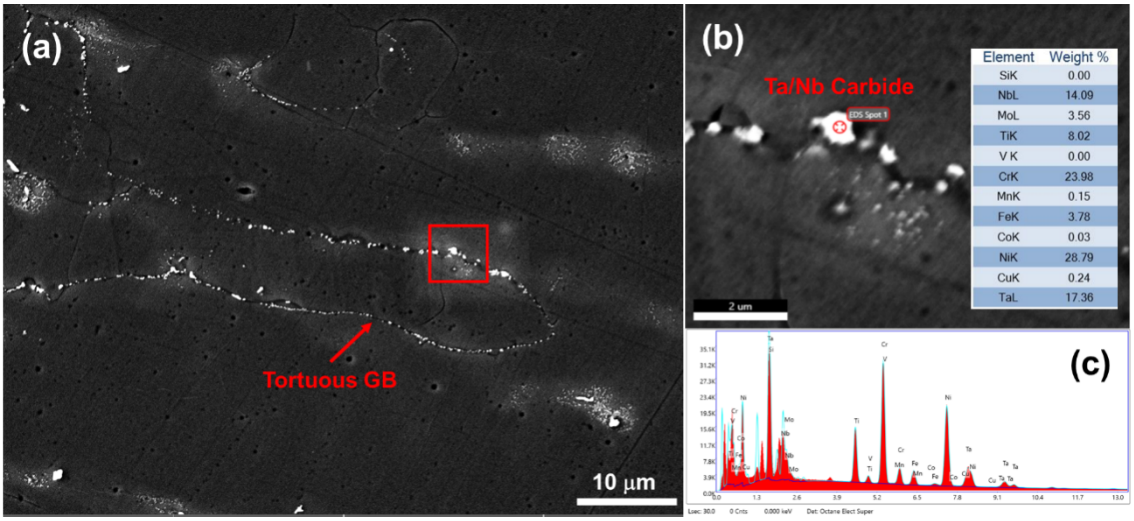


*Figure 8: SEM and EDS analyses show Ta/Nb carbides along the tortuous grain boundaries*

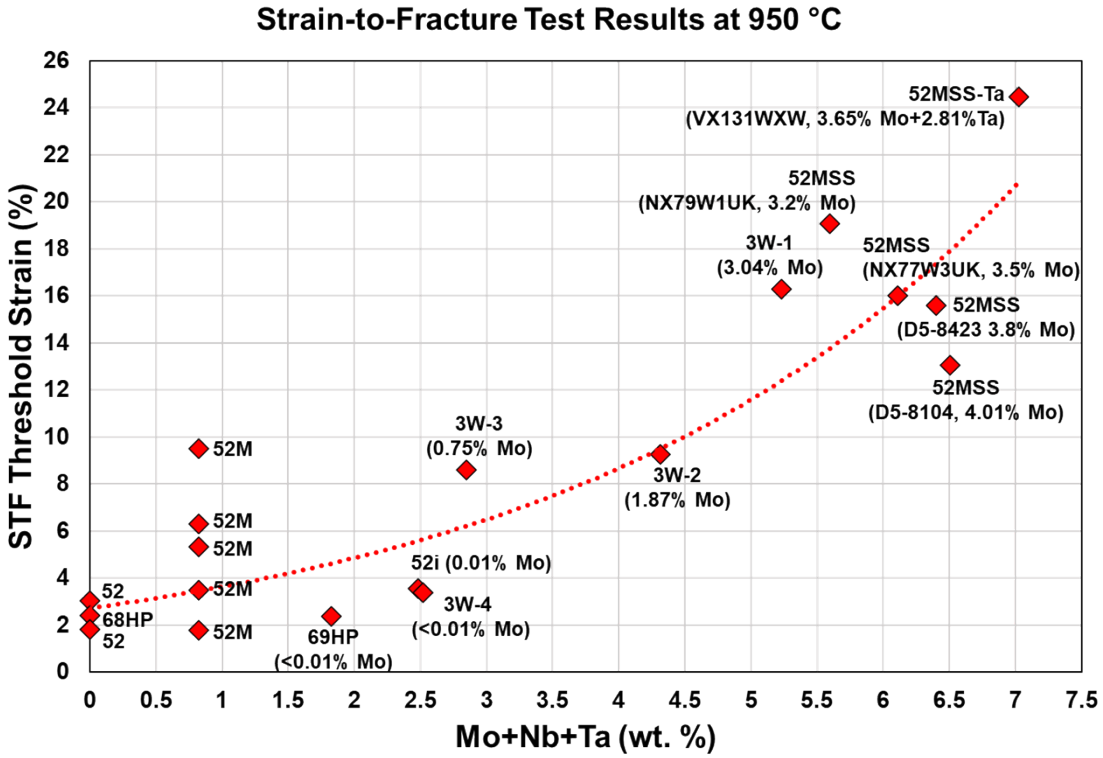


*Figure 9: Comparison of strain-to-fracture test results among different filler metals (Data source: Filler Metals 52 and 82,Filler Metal 52M Filler Metal 52MSS from (Ref. 28), Filler Metal 52M from (Ref. 16); 3W-1, 3W-2, 3W-3, 3W-4 from (Ref. 23); Filler Metals 52i,68HP,69HP from (Ref. 27).*

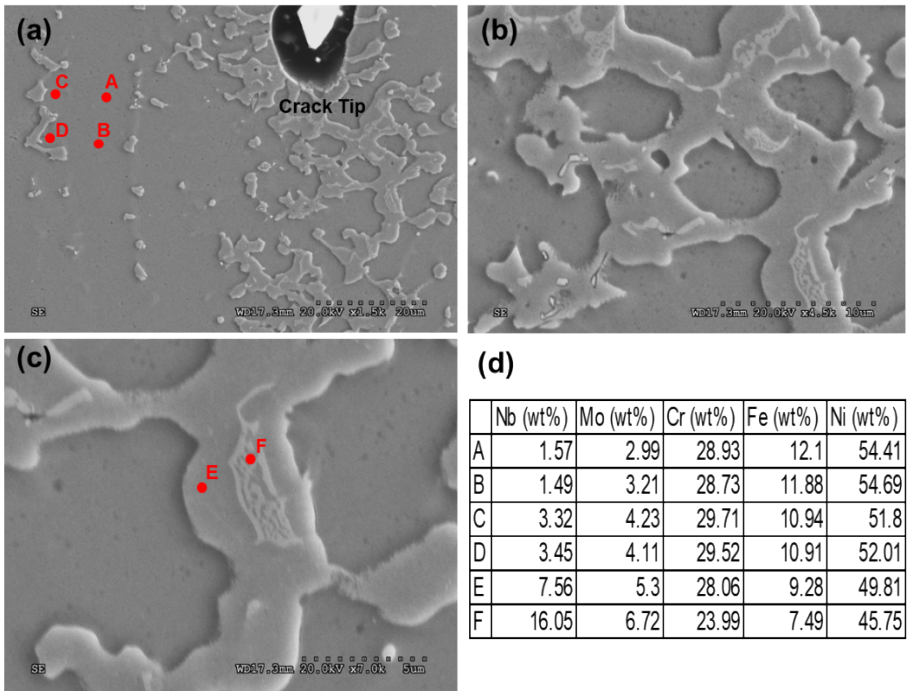


| | Nb (wt%) | Mo (wt%) | Cr (wt%) | Fe (wt%) | Ni (wt%) |
|---|---|---|---|---|---|
| A | 1.57 | 2.99 | 28.93 | 12.1 | 54.41 |
| B | 1.49 | 3.21 | 28.73 | 11.88 | 54.69 |
| C | 3.32 | 4.23 | 29.71 | 10.94 | 51.8 |
| D | 3.45 | 4.11 | 29.52 | 10.91 | 52.01 |
| E | 7.56 | 5.3 | 28.06 | 9.28 | 49.81 |
| F | 16.05 | 6.72 | 23.99 | 7.49 | 45.75 |

*Figure 10: SEM images show Laves phases induced the cracks in a LVT test sample (Filler Metal 52MSS, NX79W1UK) (Refs. 13, 28): (a) a crack tip area; (b), (c) Laves phases; (d)EDS point analysis results.*

## Tables:

**Table 1: Chemical compositions (wt.%) used for Scheil solidification simulation by Thermo-Calc**

| Elements | | Filler Metals (heat number) | | | | |
|---|---|---|---|---|---|---|
| | Filler Metal 52M | Filler Metal MSSTa Ex (HV1648) | Filler Metal MSSTa Ex (HV1673A) | Filler Metal 52MSS (NX77W3UK) | Filler Metal 52MSS (NX79W1UK) | Filler Metal 52MSS-Ta (VX131WXW) |
| C | 0.016 | 0.034 | 0.031 | 0.023 | 0.03 | 0.029 |
| Mn | 0.76 | 0.44 | 0.01 | 0.31 | 0.31 | 0.33 |
| Ni | Bal. | Bal. | Bal. | Bal. | Bal. | Bal. |
| Cr | 29.99 | 28.70 | 30.59 | 29.49 | 29.46 | 30.55 |
| Fe | 7.8 | 5.42 | 0.001 | 8.49 | 8.91 | 6.04 |
| Nb | 0.83 | 1.31 | 0.63 | 2.51 | 2.40 | 0.61 |
| Mo | 0.01 | 3.49 | 3.28 | 3.51 | 3.20 | 3.65 |
| S | 0.0007 | 0.001 | 0.001 | 0.0005 | 0.00015 | 0.0001 |
| P | 0.003 | 0.014 | 0.01 | 0.004 | 0.005 | 0.003 |
| Ti | 0.22 | 0.23 | 0.33 | 0.18 | 0.18 | 0.18 |
| Al | 0.11 | 0.29 | 0.20 | 0.13 | 0.12 | 0.048 |
| Si | 0.13 | 0.15 | 0.09 | 0.11 | 0.11 | 0.07 |
| Cu | 0.03 | 0.04 | 0.026 | 0.05 | 0.04 | 0.03 |
| Ta | - | 1.66 | 3.01 | - | - | 2.81 |

**Table 2:Verification of chemical compositions (wt.%) of 8 specimens for heat number VX131WXW**

| Sample # | C | Si | Mn | P | S | Cr | Mo | Fe | V | W | Cu | Al | Co | Nb | Ti | Ta | Pb | Ni |
|---|---|---|---|---|---|---|---|---|---|---|---|---|---|---|---|---|---|---|
| 01 | 0.029 | 0.04 | 0.33 | 0.003 | <0.001 | 29.31 | 3.41 | 7.16 | <0.02 | 0.02 | 0.03 | 0.02 | <0.005 | 0.58 | 0.26 | 2.96 | <0.005 | 55.82 |
| 02 | 0.027 | 0.04 | 0.32 | 0.003 | <0.001 | 29.59 | 3.44 | 6.62 | <0.02 | 0.02 | 0.03 | 0.02 | <0.005 | 0.58 | 0.27 | 2.89 | <0.005 | 56.13 |
| 03 | 0.027 | 0.04 | 0.32 | 0.003 | <0.001 | 29.62 | 3.44 | 6.44 | <0.02 | 0.02 | 0.03 | 0.02 | <0.005 | 0.58 | 0.28 | 3.01 | <0.005 | 56.15 |
| 04 | 0.037 | 0.04 | 0.32 | 0.003 | <0.001 | 29.32 | 3.53 | 6.38 | <0.02 | 0.02 | 0.11 | 0.03 | <0.005 | 0.61 | 0.31 | 3.05 | <0.005 | 56.24 |
| 05 | 0.028 | 0.04 | 0.32 | 0.004 | <0.001 | 29.58 | 3.43 | 6.58 | <0.02 | 0.02 | 0.03 | 0.02 | <0.005 | 0.58 | 0.28 | 3.03 | <0.005 | 56.04 |
| 06 | 0.028 | 0.04 | 0.33 | 0.004 | <0.001 | 29.59 | 3.41 | 6.69 | <0.02 | 0.02 | 0.03 | 0.02 | <0.005 | 0.57 | 0.28 | 3.04 | <0.005 | 55.92 |
| 07 | 0.029 | 0.04 | 0.33 | 0.004 | <0.001 | 29.51 | 3.44 | 6.66 | <0.02 | 0.02 | 0.03 | 0.02 | <0.005 | 0.58 | 0.29 | 3.12 | <0.005 | 55.91 |
| 08 | 0.029 | 0.04 | 0.32 | 0.004 | <0.001 | 29.66 | 3.42 | 6.62 | <0.02 | 0.02 | 0.03 | 0.02 | <0.005 | 0.57 | 0.28 | 3.05 | <0.005 | 55.91 |

**Table 3: Chemical Compositions (wt.%) of filler metals used for comparing the STF results**

| Elements | Alloys (heat number) | | | | | | | | | | | |
|---|---|---|---|---|---|---|---|---|---|---|---|---|
| | 69HP | Filler Metal 52M (EX0A51P) | 3W-1 | 3W-2 | 3W-3 | 3W-4 | 52i | Filler Metal 52MSS (D5-8423) | Filler Metal 52MSS (D5-8104) | Filler Metal 52MSS (NX77W3UK) | Filler Metal 52MSS (NX79W1UK) | Filler Metal 52MSS-Ta (VX131WXW) |
| C | 0.031 | 0.02 | 0.02 | 0.03 | 0.02 | 0.012 | 0.03 | 0.026 | 0.024 | 0.023 | 0.03 | 0.029 |
| Mn | 2.97 | 0.80 | 0.18 | 0.05 | 0.97 | 2.64 | 3.0 | 0.19 | 0.79 | 0.31 | 0.31 | 0.33 |
| Ni | 72.34 | 59.54 | 61.79 | 56.62 | 59.73 | 58.31 | Bal. | 54.67 | 53.46 | Bal. | Bal. | Bal. |
| Cr | 20.57 | 30.06 | 29.11 | 29.0 | 29.24 | 26.8 | 27 | 29.92 | 30.34 | 29.49 | 29.46 | 30.55 |
| Fe | 0.95 | 8.22 | 3.24 | 8.25 | 6.30 | 9.04 | 2.5 | 8.31 | 8.18 | 8.49 | 8.91 | 6.04 |
| Nb | 2.5 | 0.83 | 2.19 | 2.46 | 2.11 | 2.53 | 2.5 | 2.57 | 2.49 | 2.51 | 2.40 | 0.61 |
| Mo | - | 0.1 | 3.04 | 1.87 | 0.75 | <0.01 | 0.01 | 3.83 | 4.01 | 3.51 | 3.20 | 3.65 |
| S | 0.002 | 0.001 | 0.001 | 0.001 | 0.001 | 0.012 | - | 0.0013 | 0.0014 | 0.0005 | 0.00015 | 0.0001 |
| P | 0.004 | 0.003 | 0.001 | 0.003 | 0.003 | 0.006 | - | 0.0001 | 0.009 | 0.004 | 0.005 | 0.003 |
| Ti | 0.32 | 0.224 | 0.23 | 0.34 | 0.32 | 0.12 | 0.2 | 0.193 | 0.188 | 0.18 | 0.18 | 0.18 |
| Al | - | 0.11 | 0.07 | 024 | 0.22 | 0.10 | - | 0.07 | 0.218 | 0.13 | 0.12 | 0.048 |
| Si | 0.16 | 0.09 | 0.12 | 0.08 | 0.08 | 0.39 | - | 0.119 | 0.21 | 0.11 | 0.11 | 0.07 |
| Cu | 0.01 | 0.02 | 0.01 | 0.06 | 0.04 | 0.01 | - | 0.059 | 0.06 | 0.05 | 0.04 | 0.03 |
| Ta | - | - | - | - | - | - | - | - | - | - | - | 2.81 |
| Mo+Nb+Ta | 2.5 | 0.84 | 5.23 | 4.33 | 2.86 | 2.53 | 2.51 | 6.4 | 6.5 | 6.02 | 5.60 | 7.07 |

**Table 4: Spot welding parameters used for fabricating the STF specimens**

| | Time (s) | Value |
|---|---|---|
| Shielding gas pre-flow | 10 | 20 $ft^3/h$ |
| Initial current | 0.1 | 20 A |
| Upslope | 5 | 24 A/s |
| Weld current | 2.0 | 140 A |
| Downslope | 20 | 9.5 A/s |
| Final current | 0.1 | 7 A |
| Shielding gas postflow | 20 | 15 $ft^3/h$ |
| Voltage | Through the welding | ~13 V |
| Arc length | Through the welding | 0.15 inch |
| Magnetic field current | Through the welding | 0.30 A |
| Magnetic field current | Through the welding | 1.3 V |
| Tungsten stick-out | - | 8.5 mm |
| Shielding gas | Argon 99.98% | |

**Table 5: STF testing parameters used in this work**

| **Testing Steps** | **Parameters** | **Values** |
|---|---|---|
| 1 | Heating rate (°C/s) | 250-950 °C @50 °C/s |
| | | 250-800 °C @100 °C/s<br>800-950 °C @25 °C/s |
| 2 | Peak temperature (°C) | 950 |
| 3 | Dwell time at peak temperature (s) | 10 |
| 4 | Stroke (mm) | Controlled strain (selected values) |
| 5 | Stroke rate (cm/s) | 0.06 |
| 6 | Cooling rate (°C/s) | ~1 (free cool) |

**Table 6: Critical solidification temperatures and phase fractions predicted by the Scheil model using Thermo-Calc**

| Materials (heats) | $T_L$ (°C) | $T_{S\text{-effective-}0.98}$ (°C) | $\Delta T_{0.98\text{-fs}}$ (°C) | MC* (%) | Laves* (%) | Fe (wt.%) | Nb (wt.%) | Ta (wt.%) |
|---|---|---|---|---|---|---|---|---|
| Filler Metal 52M | 1377 | 1254 | 123 | 0.12 | 0.00 | 7.8 | 0.83 | 0 |
| MSSTa Ex (HV1648) | 1356 | 1105 | 251 | 0.27 | 0.24 | 5.42 | 1.31 | 1.66 |
| MSSTa Ex (HV1673A) | 1362 | 1151 | 211 | 0.24 | 0.08 | 0.001 | 0.63 | 3.01 |
| Filler Metal 52MSS-Ta (VX131WXW) | 1355 | 1108 | 247 | 0.23 | 0.24 | 6.04 | 0.61 | 2.81 |
| Filler Metal 52MSS (NX79W1UK) | 1355 | 1131 | 224 | 0.26 | 0.67 | 8.91 | 2.4 | 0 |
| Filler Metal 52MSS (NX77W3UK) | 1353 | 1125 | 228 | 0.20 | 0.77 | 8.49 | 2.51 | 0 |
| * Mole fraction of MC and Laves at 99% solid | | | | | | | | |

**Table 7: Strain-to-fracture results of the Heat Filler Metal 52MSS-Ta (VX131WXW)**

| Sample (weld spot) | Stroke | Heating process | Strain between indents | Strain between shoulders | Number of cracks <0.5mm | Number of cracks 0.5-1mm |
|---|---|---|---|---|---|---|
| 21-31 | 4mm | 250-950 °C @50 °C/s | 15.46% | 10.43% | weld spot 21: 0; weld spot 31: 1 (<0.2mm) | weld spot 21: 0; weld spot 31: 0 |
| 22-32 | 5mm | 250-950 °C @50 °C/s | 14.21% | 11.20% | weld spot 22: 1; weld spot 32: 1 | weld spot 22: 1; weld spot 32: 0 |
| 23-33 | 6mm | 250-950 °C @50 °C/s | 22.66% | 18.10% | weld spot 23: 0; weld spot 33: 0 | weld spot 23: 0; weld spot 33: 0 |
| 24-34 | 6mm | 250-850 °C @100 °C/s, 850-950C @25C/s | 29.08% | 20.10% | weld spot 24: 0; weld spot 34: 6 | weld spot 24: 0; weld spot 34: 0 |
| 25-35 | 5mm | 250-800 °C @100 °C/s, 800-950 °C @25C/s | 19.18% | 13.71% | weld spot 25 0; weld spot 35: 0 | weld spot 25 0; weld spot 35: 0 |
| 26-36 | 6mm | 250-800 °C @100 °C/s, 800-950 °C @25 °C/s | 25.73% | 20.96% | weld spot 26: 4; weld spot 36: 0 | weld spot 26: 5; weld spot 36: 0 |
| 27-37 | 5.5mm | 250-800 °C @100 °C/s, 800-950 °C @25 °C/s | 20.69% | 17.22% | weld spot 27: 0; weld spot 37: 0 | weld spot 27: 0; weld spot 37: 1 |
| 28-38 | 5.5mm | 250-800 °C @100 °C/s, 800-950 °C @25 °C/s | 25.72% | 17.44% | weld spot 28: 1; weld spot 38: 0 | weld spot 28: 3; weld spot 38: 0 |
| 29-39 | 5.5mm | 250-800 °C @100 °C/s, 800-950 °C @25 °C/s | 24.19% | 18.10% | weld spot 29: 0; weld spot 39: 0 | weld spot 29: 0; weld spot 39: 0 |
| 30-40 | 5.25mm | 250-800 °C @100 °C/s, 800-950 °C @25 °C/s | 22.04% | 17.10% | weld spot 30: 0; weld spot 40: 0 | weld spot 30: 3; weld spot 40: 0 |